



Optimal deployment of public charging stations for plug-in hybrid electric vehicles

Fang He^a, Di Wu^a, Yafeng Yin^{a,*}, Yongpei Guan^b

^a Department of Civil and Coastal Engineering, University of Florida, 365 Weil Hall, Gainesville, FL 32611-6580, United States

^b Department of Industrial and Systems Engineering, University of Florida, 303 Weil Hall, Gainesville, FL 32611-6595, United States

ARTICLE INFO

Article history:

Received 2 December 2011

Received in revised form 29 September 2012

Accepted 29 September 2012

Keywords:

Plug-in hybrid electric vehicles

Equilibrium

Price of electricity

Public charging stations

Social welfare

ABSTRACT

This paper develops an equilibrium modeling framework that captures the interactions among availability of public charging opportunities, prices of electricity, and destination and route choices of plug-in hybrid electric vehicles (PHEVs) at regional transportation and power transmission networks coupled by PHEVs. The modeling framework is then applied to determine an optimal allocation of a given number of public charging stations among metropolitan areas in the region to maximize social welfare associated with the coupled networks. The allocation model is formulated as a mathematical program with complementarity constraints, and is solved by an active-set algorithm. Numerical examples are presented to demonstrate the models and offer insights on the equilibrium of the coupled transportation and power networks, and optimally allocating resource for public charging infrastructure.

© 2012 Elsevier Ltd. All rights reserved.

1. Introduction

Electric vehicles have been long recognized as a promising way to reduce traffic emissions locally and petroleum dependence. Early models of electric vehicles all came with limitations and costs that prevented them from competing with gas-fueled cars. However, recent advances in battery technologies and expeditiously rising prices of crude oil have helped re-launch electric vehicles. Among the emerging models, plug-in hybrid electric vehicles (PHEVs) enjoy special attention, thanks to the cost savings, flexibility and extended driving range they offer to the customers (e.g., Kalhammer et al., 2009; Markel, 2010). PHEVs are vehicles with a battery storage system of 4 kW h or more, a means of recharging the battery from an external source and the ability to drive at least 10 miles in all-electric mode (IEEE, 2007). The powertrain of a PHEV consists of an electric motor, an internal combustion engine and a plug to connect to the power grid. In a range-extended design, a PHEV operates in an all-electric mode and draws propulsion energy entirely from the battery until it reaches the target state of charge. The vehicle then switches to a charge-sustaining mode and the gasoline engine provides energy to propel the vehicle and maintains battery charge near the target state of charge (e.g., Bradley and Frank, 2009). Loosely speaking, if the battery's charge is sufficient, the vehicle operates as an all-electric vehicle like Nissan Leaf, while in a charge-sustaining mode it is effectively a hybrid electric vehicle like Toyota Prius. Compared to the latter, PHEVs offer more fuel savings due to their much larger battery, which can be recharged at home from typical 110 V or 220 V outlets. PHEVs provide extended driving range and eliminate the "range anxiety" that kept customers away from all-electric vehicles (Markel, 2010). Recognizing the potentials of PHEVs, many governments have plans to promote the deployment of PHEVs. For example, the Obama Administration in the US has proposed to put a total of one million PHEVs on road by 2015 (Obama, 2008).

* Corresponding author. Tel.: +1 352 392 9537x1455; fax: +1 352 392 3394.

E-mail address: yafeng@ce.ufl.edu (Y. Yin).

Although currently most PHEVs in the US are conversions of conventional hybrid electric vehicles, major vehicle manufacturers, including Toyota, General Motors and Ford, have their PHEVs available in the market starting 2011 (Rotering and Ilic, 2011). A fast-growing adoption of PHEVs can be expected.

With the existing charging technologies, PHEVs are generally plugged into 110 V or 220 V outlets for a few hours to fully recharge their batteries. Although these charging activities mostly take place at home and work places (e.g., Davies and Kurani, 2010), providing public charging infrastructures is critical for the growth of the PHEV market (Morrow et al., 2008). Many governments are planning to deploy public charging stations in their regions. For example, California announced to build 200 public fast-charging stations and wire for 10,000 plug-in units at 1000 locations across the state. British Columbia, Canada, has a plan of building 570 charging stations across the province (GLOBLE-Net, 2012). Important decisions in deploying those charging stations will include, among others, allocating a number of charging stations to metropolitan areas, and determining locations of the allocated charging stations and their corresponding capacities.

A few studies have investigated locating public charging stations in metropolitan areas. Frade et al. (2010) formulated a maximum covering model to locate a certain number of charging stations to maximize the demand covered within a given distance. Ip et al. (2010) first applied a hierarchical clustering analysis to identify the demand clusters of PHEVs and then formulated simple assignment models to locate charging stations to those demand clusters. Pan et al. (2010) developed a two-stage stochastic program to optimally locate PHEV battery swapping stations prior to the realization of battery demands, loads and generation capacity of renewable power sources. Finally, Sweda and Klabjan (2011) developed an agent-based decision support system for electric vehicle charging infrastructure deployment.

The above studies ignore the interactions between transportation and power systems, which are coupled by PHEVs (e.g., Galus and Andersson, 2008; Kezunovic et al., 2010). Generally speaking, the policies and measures implemented in the transportation system will change the spatial and temporal distribution of PHEVs and thus the pattern of their energy requirement, thereby affecting the operations of the power system. On the other hand, the provision of the charging infrastructure and the associated charging strategies and expenses will affect the travel patterns of PHEVs and consequently the operations of the transportation system. Using Pennsylvania–New Jersey–Maryland Interconnection as a case study, Wang et al. (2010) demonstrated that, under existing charging infrastructures, even a small magnitude of load increase caused by PHEV charging activities can have a significant undesirable impact on the electricity price. The impact could be mitigated to a varying extent by advanced controls based on future charging infrastructures. Wehinger et al. (2010) pointed out that the timing of PHEV charging has a major impact on market prices of electricity. If PHEVs are mainly charged during off-peak hours, the daily load curve would be flattened and the volatility of hourly price of electricity can be reduced. These studies in the power engineering field have demonstrated the influence of PHEV charging loads on the spatial and temporal difference of market prices of electricity. More recently, Sioshansi (2012) examined the impacts of electricity price on PHEV drivers' charging decisions, and compared the costs and emissions under different price structures and the ideal case of charging controlled by the system operator.

For the deployment planning of public charging infrastructure, it is thus of importance to consider the interplay between transportation and power systems, which is expected to be multifaceted and thus difficult to model. We envision a hierarchical modeling structure where a strategic planning model captures the interactions between regional transportation network and transmission power grid to determine the optimal allocation plan of charging stations while a tactic planning model focuses on the interconnectivity between urban transportation network and power distribution network to optimize the locations and capacities of charging stations in a metropolitan area. This paper reports our effort to construct a strategic planning model. More specifically, we adopt a static game theoretical approach to investigate the interactions among availability of public charging stations, destination choices of PHEVs, and prices of electricity. The interactions lead to an equilibrium in the coupled transportation and power networks where prices of electricity, and traffic and power flow distributions can be determined. We formulate the equilibrium conditions into a convex mathematical program. We then examine how to allocate public charging stations to maximize the social welfare associated with the coupled networks.

For the remainder, Section 2 describes the transportation and power networks and examines the equilibrium state in the coupled networks. A mathematical program is developed to estimate the equilibrium prices of electricity and flow distributions on both networks. Incorporating the equilibrium conditions as constraints, Section 3 formulates finding an optimal allocation of public charging stations as a mathematical program with complementarity constraints, and then proposes its solution algorithm. Section 4 presents a numerical example to demonstrate the allocation model. Lastly, Section 5 concludes the paper.

2. Equilibrium of coupled transportation and power networks

2.1. Description of transportation network

We consider a regional road network where origins and destinations are cities or metropolitan areas. A large portion of vehicles in the network are assumed to be PHEVs, and other vehicles are reflected as the background traffic. We attempt to model the spatial distribution of travel demand of PHEVs and their corresponding route choices in the regional network. Previous studies, e.g., Tuttle and Kockelman (2012) and Lin and Greene (2011), have suggested that drivers of PHEVs actively

seek out charging opportunity to avoid gasoline use and thus favor a destination that provides public charging facilities. This explains why hotels and shopping malls have been installing charging stations as their amenities (e.g., Fox News, 2012). Moreover, considering the way how fuel prices affect travel behaviors (e.g., Walsh et al., 2004; Weis et al., 2010), it seems reasonable to assume that the charging price will have a similar effect. Kitamura and Sperling (1987) analyzed the refueling behaviors of drivers of gas-fueled vehicles and found that price of gasoline is a primary concern of a majority of drivers for selecting fuel stations. Similarly, it is plausible that the charging expense will be one important criterion for drivers of PHEVs to select charging stations, particularly if the prices of electricity vary substantially among stations. The above behaviors and preferences will likely manifest themselves in shaping the spatial distribution of travel demand of PHEVs in the region. To reflect their impact, we assume in this paper that among other factors, drivers of PHEVs consider travel time, availability of charging opportunities, and charging expense in selecting destinations. We caution that this is a critical assumption that needs to be verified by future empirical studies. It is further assumed that the above destination choice behavior can be captured by a multinomial logit model, and drivers select routes in a user optimum manner. Note that multinomial logit models have been applied to predict travelers' destination choices in large urban and regional systems (e.g., Southworth, 1981; Kemperman et al., 2002), and the assumption of user-optimum route choice has been widely adopted in transportation network modeling (e.g., Sheffi, 1984).

2.1.1. Notation

Let $GT(N, A)$ denote the network of roads, where N and A are the sets of nodes and links in the network respectively. We denote a link as $a \in A$ or the pair of its starting and ending nodes, i.e., $a = (i, j) \in A$. Assume that the travel demands of interest are originated from a set of origin nodes $R \subseteq N$, and denote the demand at each origin as d^r , $r \in R$. Next, let $S \subseteq N$ denote a set of destinations, where sit public charging stations for PHEVs. Note that the sets R and S are not mutually exclusive. We use an integer variable y_c^s to represent the number of charging stations at destination s .

Let A be the node-link incidence matrix associated with the network and E^{rs} is a vector with a length of $|R| \times |S|$. The vector consists of two non-zero components: one has a value of 1 in the component corresponding to origin r and the other has a value of -1 in the component corresponding to destination s . The origin-destination (O-D) flows, i.e., q^{rs} , are the results from travelers' destination choices, and thus are decision variables in the network flow model.

Let v_a be the link flow at link a . Since only a portion of travel demand is of consideration, there exists background traffic in the network. Without losing generality, we hereinafter assume the background traffic to be zero,¹ and the travel time t_a for link a is a strictly increasing function of the PHEV flow on the link, i.e., $t_a(v_a)$. For example, the following form of Bureau of Public Roads (BPR) function can be used:

$$t_a = t_a^0 \left[1 + 0.15 \left(\frac{v_a}{c_a} \right)^4 \right]$$

where t_a^0 is the free-flow travel time for link a and c_a is the capacity of link a .

2.1.2. Combined distribution and assignment model

We now model the travel demand distribution of PHEVs, given the availability of charging stations and price of electricity at each destination. A combined distribution and assignment (CDA) model is proposed to describe PHEVs' choices of destinations and routes. In the CDA model, the network traffic condition is assumed to be in user equilibrium and the destination choice is represented by a multinomial logit model as follows:

$$\frac{q^{rs}}{d^r} = \frac{\exp(-\alpha t^{rs} + \beta A_s^{-1} y_c^s - \gamma p^s e^{rs} + \theta^s)}{\sum_{s \in S} \exp(-\alpha t^{rs} + \beta A_s^{-1} y_c^s - \gamma p^s e^{rs} + \theta^s)}$$

where α , β and γ are positive coefficients associated with the O-D equilibrium travel time, i.e., t^{rs} , the density of charging stations at the destination, which equals the number of charging stations, i.e., y_c^s , divided by the area of the destination, i.e., A_s , and the charging expense, which is equal to the unit price, i.e., p^s multiplied by the average hourly energy requirement for a PHEV, i.e., e^{rs} . The latter is assumed to be a constant for each OD pair (e.g., Wang et al., 2011). θ^s is a location-specific constant. For presentation simplicity, we hereinafter substitute β^s for βA_s^{-1} . Note that if $r = s$, q^{rr} represents the intra-zone travel demand.

The above logit model implies that the deterministic portion of the utility function of PHEV drivers consists of four components: travel time, the availability of charging opportunities, charging expense and a constant that encapsulates other factors affecting the attractiveness of a particular destination. With such a consideration of destination choices, the CDA model can be written as follows:

¹ It is straightforward to extend the modeling framework in this paper to consider multiple user classes if modeling travel choices of the background traffic is of interest.

$$\min_{x, v, q} \sum_a \int_0^{v_a} t_a(w) dw + \frac{1}{\alpha} \sum_r \sum_s q^{rs} (\ln q^{rs} - 1) + \frac{1}{\alpha} \sum_r \sum_s (\gamma p^s e^{rs} - \beta^s y_c^s - \theta^s) q^{rs}$$

$$\text{s.t. } v_a = \sum_{rs} x_a^{rs} \quad \forall a \in A \quad (1)$$

$$\Delta x^{rs} = E^{rs} q^{rs} \quad \forall r \in R, s \in S \quad (2)$$

$$\sum_s q^{rs} = d^r \quad \forall r \in R \quad (3)$$

$$x_a^{rs} \geq 0 \quad \forall a \in A, r \in R, s \in S \quad (4)$$

$$q^{rs} \geq 0 \quad \forall r \in R, s \in S \quad (5)$$

where x_a^{rs} is the flow between the O–D pair (r, s) at link a . Constraint (1) calculates the aggregate link flow. Constraint (2) ensures the flow balance between origin and destination nodes in the network. Constraint (3) requires the sum of the demand leaving from any origin r to each destination s to be equal to the total demand generated at that particular origin r . Constraint (4) and (5) are the non-negativity constraints for the link flows and demands. Constraints (1)–(5) essentially define a set of feasible O–D and link flow distributions for the network.

Lastly, we emphasize that the coefficients in the above multinomial logit model need to be calibrated using empirical stated or revealed preference data, which may prove some of the parameters to be insignificant. Between the availability of charging opportunities and the price of electricity, the former more likely affects travel choices of PHEV drivers, as suggested in previous studies (e.g., Lin and Greene, 2011). In contrast, the impact of the price of electricity may be less significant because the price may not vary substantially across locations or even if it does, it may not yield a meaningful difference in the total charging expense per charge. If neither the availability of public charging opportunities nor the price of electricity has been proved to be strong enough in shaping the O–D demand distribution of PHEVs, the coefficients, γ and β , will become zero, and the CDA model will consequently reduce to a traditional combined distribution and assignment mode (e.g., Sheffi, 1984). If another form of the utility function provides a better fit with the data, a corresponding CDA model can be developed in a similar fashion.

2.2. Description of power network

2.2.1. Configuration of the wholesale power market

We consider a competitive wholesale power market, consistent with the one proposed by the US Federal Energy Regulatory Commission (FERC, 2003). In the market, an independent system operator (ISO) undertakes the daily operations of the transmission grid using locational marginal pricing. More specifically, the ISO accepts supply and demand bids submitted by market participants, i.e., buyers and generators, and is responsible for determining the power commitments (supplies) to meet the demands, with an objective of maximizing social welfare while ensuring the system security. In this case, the price of electricity at each location equals the marginal cost of providing electricity at that location, i.e., the locational marginal price (LMP). LMP reflects the market clearing price at each location. Based on their LMPs, the buyers pay the ISO for the dispatched power (e.g., Sun and Tesfatsion, 2010).

We assume in this paper that the retail electricity prices faced by the PHEV drivers at different public charging stations in the same destination are the same and equal to the LMP at the specific location. We further assume that there are a variety of active participants in the wholesale power market, leading LMP to vary substantially by location (e.g., Lewis, 2010 and Feldman (2012)). The spatial variability of LMP will influence travel patterns of PHEVs, which in return has significant impacts on LMPs and the operations of the power network.

2.2.2. Calculation of LMP

The clustered PHEV loads at public charging stations will have attendant effects on LMPs of electricity, which can be estimated by solving an optimal power flow problem. All current market designs utilize the DC power flow models for LMP calculation, which are linear approximations to the AC models (e.g., Litvinov et al., 2004). Although the approximations lead to some loss of accuracy, the results match fairly closely with the full AC solutions (Overbye et al., 2004).

This paper adopts the standard DC power flow model to compute the LMP at each bus, including the destinations with public charging stations. Without losing generality, we assume that there are only one generator and one buyer at each bus. Public charging stations for PHEVs will create additional electricity load to the bus at their particular locations.

Let $GP(K, L)$ denote the power network, where K and L are the sets of buses and transmission lines in the network respectively. For the generator at bus $k \in K$, g_k is the real power injection, and LG_k and UG_k represent the lower and upper real power limit respectively. We further denote a transmission line or branch as the pair of its starting and ending buses, i.e., $(k, m) \in L$. For each branch, let f_{km} represent the real power flowing in the branch and U_{km} represent the thermal limit of real power flow. The standard DC power flow model is written as follows:

$$\begin{aligned}
& \min_{g, f, \delta} \sum_k c_k(g_k) \\
& \text{s.t. } g_k - l_k - \hat{l}_k - \sum_{(k,m) \in L} f_{km} = 0 \quad \forall k \in K \quad (6) \\
& f_{km} = B_{km}(\delta_k - \delta_m) \quad \forall (k, m) \in L \quad (7) \\
& f_{km} \geq -U_{km} \quad \forall (k, m) \in L \quad (8) \\
& f_{km} \leq U_{km} \quad \forall (k, m) \in L \quad (9) \\
& g_k \geq LG_k \quad \forall k \in K \quad (10) \\
& g_k \leq UG_k \quad \forall k \in K \quad (11) \\
& \delta_1 = 0 \quad (12)
\end{aligned}$$

where $c_k(g_k)$ is the total cost of generating g_k amount of electricity at bus k , which is assumed to be a strictly convex function with g_k , l_k is the regular real power load at bus k , which is given.² \hat{l}_k is the additional load created by PHEVs, defined as follows: $\hat{l}_k = \sum_{(s,k) \in C} \sum_r q^{rs} \cdot e^{rs}$, where C denotes the set of the pairs of travel destinations and their serving buses. B_{km} is the inverse of the pu reactance and δ_k is the multiplication of the base apparent power and voltage angle (in radians).

In the above, constraint (6) is the nodal power balance constraint, whose associated Lagrangian multiplier is the LMP at the node. Constraint (7) is the linear real power branch flow equation. Constraints (8)–(11) ensure the feasibility of the real power flow and power injection. Lastly, constraint (12) sets the voltage angle at the reference node 1 to be 0.

2.3. Equilibrium of coupled transportation and power networks

The interactions between destination choices of PHEVs and price of electricity will lead to an equilibrium state in the coupled networks. The state implies a market equilibrium where the supply of electricity matches its demand so that the price of electricity and the power flow can consequently be determined. The state also encapsulates a user equilibrium in the transportation network where no PHEV is able to improve its perceived utility by unilaterally changing its route or destination.

2.3.1. Mathematical definition

Combining the KKT conditions of the CDA and DC power flow models yields a mathematical definition of the equilibrium state in the coupled networks. The definition is a non-linear complementarity system as follows:

$$(1) - (12) \quad (t_{ij} - \rho_i^{rs} + \rho_j^{rs}) \cdot x_{ij}^{rs} = 0 \quad \forall (i, j) \in A, r \in R, s \in S \quad (13)$$

$$t_{ij} - \rho_i^{rs} + \rho_j^{rs} \geq 0 \quad \forall (i, j) \in A, r \in R, s \in S \quad (14)$$

$$\frac{1}{\alpha} (\ln q^{rs} + \gamma p^s e^{rs} - \beta^s y_c^s - \theta^s) + \rho_r^{rs} - \rho_s^{rs} - \tau^r = 0 \quad \forall r \in R, s \in S \quad (15)$$

$$\bar{c}_k(g_k) - p_k - \kappa_k^o + \kappa_k^u = 0 \quad \forall k \quad (16)$$

$$\kappa_k^o(g_k - LG_k) = 0 \quad \forall k \quad (17)$$

$$\kappa_k^u(g_k - UG_k) = 0 \quad \forall k \quad (18)$$

$$\kappa_k^o, \kappa_k^u \geq 0 \quad \forall k \quad (19)$$

$$p^k - \varpi_{km} - \theta_{km}^o + \theta_{km}^u = 0 \quad \forall (k, m) \in L \quad (20)$$

$$\theta_{km}^o(f_{km} + U_{km}) = 0 \quad \forall (k, m) \in L \quad (21)$$

$$\theta_{km}^u(f_{km} - U_{km}) = 0 \quad \forall (k, m) \in L \quad (22)$$

$$\theta_{km}^o, \theta_{km}^u \geq 0 \quad \forall (k, m) \in L \quad (23)$$

$$\sum_{(k,m) \in L} B_{km} \varpi_{km} - \sum_{(m,k) \in L} B_{mk} \varpi_{mk} = 0 \quad \forall k; k \neq 1 \quad (24)$$

$$\sum_{(1,m) \in L} B_{1m} \varpi_{1m} - \sum_{(m,1) \in L} B_{m1} \varpi_{m1} - \zeta = 0 \quad (25)$$

where ρ_i^{rs} is the Lagrangian multiplier associated with constraint (2), τ^r with constraint (3), p^k with constraint (6), ϖ_{km} with constraint (7), θ_{km}^o with constraint (8), θ_{km}^u with constraint (9), κ_k^o with constraint (10), κ_k^u with constraint (11) and ζ with constraint (12). Moreover, $\bar{c}_k(g_k)$ is the marginal generation cost at bus k .

Below we present an example with a three-node road network and a three-bus power network to illustrate the equilibrium concept. As shown in Fig. 1, the road network consists of nodes 1, 2 and 3 where 5000 PHEVs generated at node 1 are destined to the other two nodes. There are three and five public charging stations at nodes 2 and 3 respectively, whose serving buses compose the power grid with another bus, i.e., 4. There is no electricity load at bus 4, and the regular load at buses

² If the regular real power load is not given and needs to be treated as a decision variable, its corresponding (inverse) demand function should be specified. Consequently, the objective function of the DC power flow model will be changed to maximizing social benefit.

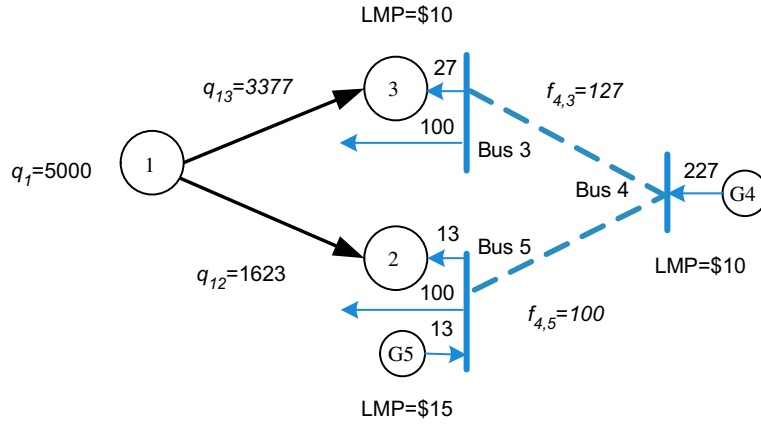


Fig. 1. An illustrative example for equilibrium in coupled networks.

3 and 5 are both 100 MW. It is assumed that the total generation cost functions at buses 4 and 5 are linear and the unit costs are \$10 and \$15 per MWh respectively. We use the BPR function to calculate the travel time of links 1–2 and 1–3, whose free-flow travel times and capacities are both 60 min and 4000 veh/hr respectively. Other parameters are assumed as follows: $\alpha = 1$; $\gamma = 0.1$; $\beta^s = 0.4$; $\theta = 0$; $U_{45} = 100$ MW; $U_{43} = 200$ MW; $B_{km} = 4$ pu; $UG_4 = 250$ MW; $UG_5 = 100$ MW; $UG_3 = 0$; $LG_k = 0$ and $e^{rs} = 8.25$ kW h.

We solved (1)–(25) for the illustrative network to obtain the equilibrium solution. At equilibrium, 3377 PHEVs leave from node 1 to 3, generating additional electricity load of 27 MW and facing a LMP of \$10 per MWh. The other 1623 PHEVs leaving for node 2 create electricity load of 13 MW at a price of \$15 per MWh. The power injections at buses 4 and 5 are 227 MW and 13 MW respectively.

2.3.2. Equivalent mathematical program

Instead of solving the non-linear complementarity system (1)–(25), this section presents a convex mathematical program whose solution is the equilibrium O–D demands and link flows (or simply traffic flow distribution) at the transportation network, and the power injection and branch flow (or simply power flow distribution) at the power network. We hereinafter refer to it as the network equilibrium problem, i.e., NEP, and the formulation is as follows:

$$\begin{aligned} \min_{(x,q,v,g,\delta,f)} \quad & \frac{\alpha}{\gamma} \sum_a \int_0^{v_a} t_a(\varpi) d\varpi + \frac{1}{\gamma} \sum_r \sum_s q^{rs} (\ln q^{rs} - 1) + \frac{1}{\gamma} \sum_r \sum_s (-\beta^s y_c^s - \theta^s) q^{rs} + \sum_k c_k(g_k) \\ \text{s.t.} \quad & (1)–(12) \end{aligned}$$

The equivalence of NEP to the equilibrium definition (1)–(25) can be easily established by examining the KKT condition of NEP as follows:

$$\begin{aligned} & (1)–(12) \\ & \left(\frac{\alpha}{\gamma} t_{ij} - \hat{\rho}_i^{rs} + \hat{\rho}_j^{rs} \right) \cdot x_{ij}^{rs} = 0 \quad \forall (i,j) \in A, r \in R, s \in S \\ & \frac{\alpha}{\gamma} t_{ij} - \hat{\rho}_i^{rs} + \hat{\rho}_j^{rs} \geq 0 \quad \forall (i,j) \in A, r \in R, s \in S \\ & \frac{1}{r} (\ln q^{rs} - \beta^s y_c^s - \theta^s) + \hat{\rho}_r^{rs} - \hat{\rho}_s^{rs} - \hat{\tau}^r + e^{rs} \cdot p^k = 0 \quad \forall r \in R, s \in S, (s,k) \in C \\ & \bar{c}_k(g_k) - \hat{p}^k - \hat{\kappa}_k^o + \hat{\kappa}_k^u = 0 \quad \forall k \\ & \hat{\kappa}_k^o(g_k - LG_k) = 0 \quad \forall k \\ & \hat{\kappa}_k^u(g_k - UG_k) = 0 \quad \forall k \\ & \hat{\kappa}_k^o, \hat{\kappa}_k^u \geq 0 \quad \forall k \\ & \hat{p}^k - \hat{\omega}_{km} - \hat{\theta}_{km}^o + \hat{\theta}_{km}^u = 0 \quad \forall (k,m) \in L \\ & \hat{\theta}_{km}^o(f_{km} + U_{km}) = 0 \quad \forall (k,m) \in L \\ & \hat{\theta}_{km}^u(f_{km} - U_{km}) = 0 \quad \forall (k,m) \in L \\ & \hat{\theta}_{km}^o, \hat{\theta}_{km}^u \geq 0 \quad \forall (k,m) \in L \\ & \sum_{(k,m) \in L} B_{km} \hat{\omega}_{km} - \sum_{(m,k) \in L} B_{mk} \hat{\omega}_{mk} = 0 \quad \forall k; k \neq 1 \\ & \sum_{(1,m) \in L} B_{1m} \hat{\omega}_{1m} - \sum_{(m,1) \in L} B_{m1} \hat{\omega}_{m1} - \hat{\zeta} = 0 \end{aligned}$$

where $\hat{\rho}_i^{rs}$ is the Lagrangian multiplier associated with constraint (2) in NEP, $\hat{\tau}^r$ with constraint (3), \hat{p}^k with constraint (6), $\hat{\omega}_{km}$ with constraint (7), $\hat{\theta}_{km}^o$ with constraint (8), $\hat{\theta}_{km}^u$ with constraint (9), $\hat{\kappa}_k^c$ with constraint (10), $\hat{\kappa}_k^u$ with constraint (11) and $\hat{\zeta}$ with constraint (12).

Comparing the above KKT conditions to the definition of equilibrium, i.e., (1)–(25), one can find that these two systems are the same except that $\hat{\rho}_i^{rs}$ and $\hat{\tau}^r$ are $\frac{\alpha}{\gamma}$ times of ρ_i^{rs} and τ^r in (1)–(25). More specifically, the solutions to NEP, i.e., the traffic and power flow distributions, satisfy the equilibrium definitions (1)–(25) and the equilibrium prices of electricity are the Lagrangian multipliers associated with constraint (6) in NEP.

Theorem 1. *Given the availability of public charging stations, the equilibrium state always exists. The equilibrium traffic link flows, O–D demand distributions and real power injections are unique.*

Proof. As the objective function of NEP is continuous and its feasible region is compact and non-empty, according to Weierstrass's Theorem (e.g., Bertsekas, 2003), there must exist a solution to NEP. In other words, equilibrium always exists in the coupled networks.

Define the convex feasible region of NEP as Φ , and thus its solution $(x^*, v^*, q^*, g^*, \delta^*, f^*)^T$ will satisfy the following first-order optimality condition:

$$\sum_a \frac{\alpha}{\gamma} t_a(v_a^*)(v_a - v_a^*) + \sum_{(r,s)} \frac{1}{r} (\ln q^{rs*} - \beta^s y_c^s - \theta^s)(q^{rs} - q^{rs*}) + \sum_k \bar{c}_k(g_k^*)(g_k - g_k^*) \geq 0 \quad \forall (x, v, q, g, \delta, f)^T \in \Phi \quad (26)$$

Suppose that there are two optimal solutions, and denote them as $(x^1, v^1, q^1, g^1, \delta^1, f^1)^T$ and $(x^2, v^2, q^2, g^2, \delta^2, f^2)^T$. Substituting them into (26) yields the following:

$$\sum_a \frac{\alpha}{\gamma} t_a(v_a^1)(v_a^2 - v_a^1) + \sum_{(r,s)} \frac{1}{r} (\ln q^{rs1} - \beta^s y_c^s - \theta^s)(q^{rs2} - q^{rs1}) + \sum_k \bar{c}_k(g_k^1)(g_k^2 - g_k^1) \geq 0 \quad (27)$$

$$\sum_a \frac{\alpha}{\gamma} t_a(v_a^2)(v_a^1 - v_a^2) + \sum_{(r,s)} \frac{1}{r} (\ln q^{rs2} - \beta^s y_c^s - \theta^s)(q^{rs1} - q^{rs2}) + \sum_k \bar{c}_k(g_k^2)(g_k^1 - g_k^2) \geq 0 \quad (28)$$

Summing (27) and (28) leads to:

$$\sum_a \frac{\alpha}{\gamma} (t_a(v_a^1) - t_a(v_a^2))(v_a^2 - v_a^1) + \sum_{(r,s)} \frac{1}{r} (\ln q^{rs1} - \ln q^{rs2})(q^{rs2} - q^{rs1}) + \sum_k (\bar{c}_k(g_k^1) - \bar{c}_k(g_k^2))(g_k^2 - g_k^1) \geq 0 \quad (29)$$

Because the BPR, logarithm and the marginal generation cost functions are all strictly increasing, (29) implies that $v_a^2 = v_a^1$, $q^{rs2} = q^{rs1}$ and $g_k^2 = g_k^1$. In other words, $(v^*, q^*, g^*)^T$ must be unique. \square

3. Allocating public charging stations

3.1. Model formulation

With the proposed framework of equilibrium analysis of the coupled networks, we now investigate how to allocate a given number of public charging stations to a set of potential locations, a strategic decision in the deployment planning of public charging infrastructure. It is assumed that the government agency attempts to maximize social welfare associated with both the transportation and power networks. We propose a macroscopic planning model that determines the optimal number of charging stations allocated to each metropolitan area. Being strategic, the model does not optimize exact locations and capacities of the allocated charging stations, which are expected to be decided by another tactic planning model.

Defining a non-negative integer variable y^s to represent the number of additional charging stations allocated to node s , we formulate the public charging station allocation problem (PCSA) as follows:

$$\begin{aligned} \max_{(y, x, v, q, g, f, \delta, \rho, \tau, \kappa, p, \omega, \theta, \zeta)} & \frac{1}{\gamma} \sum_{r \in R} \ln \left(\sum_{s \in S} \exp [-\alpha(\rho_r^{rs} - \rho_s^{rs}) + \beta^s (y_c^s + y^s) - \gamma p^s e^{rs} + \theta^s] \right) \cdot d^r + \sum_{r \in R} \sum_{s \in S} q^{rs} p^s e^{rs} - \sum_k c_k(g_k) - \sum_{s \in S} M^s y^s \\ \text{s.t.} & (1) - (14), (16) - (25) \end{aligned} \quad (30)$$

$$\frac{1}{\alpha} (\ln q^{rs} + \gamma p^s e^{rs} - \beta^s (y_c^s + y^s) - \theta^s) + \rho_r^{rs} - \rho_s^{rs} - \tau^r = 0 \quad \forall r \in R, s \in S \quad (31)$$

$$\sum_{s \in S_p} y^s \leq I \quad (32)$$

$$\sum_{s \notin S_p} y^s = 0 \quad (32)$$

where I is the given total number of public charging stations, and S_p denotes the set of potential locations.

In the above, the objective is to maximize social welfare of the coupled networks for an average hour. It consists of four components. The first one represents the total expected utility of PHEV drivers where $\rho_r^{rs} - \rho_s^{rs}$ is the equilibrium travel time between the O–D pair $r - s$. Because the utility encapsulates the charging expense paid by PHEV drivers, which, however, should be viewed as a transfer, the second components, i.e., the charging expense, is thus added. The last two components represent the total generation cost of electricity and the total construction cost of charging stations. M^s is the construction cost of a charging station at destination s .

In the constraints, (1)–(14), (16)–(25) and (30) ensure that the traffic and power flow distributions and prices of electricity are in equilibrium. The others require the total number of located charging stations to be less than I and the charging stations can only be allocated to the potential locations. Note that by solving PCSA, not only can we obtain the allocation plan but also the equilibrium traffic distribution, which can be potentially used as inputs to the tactic planning model to determine the locations and capacities of allocated charging stations.

3.2. Solution algorithm

PCSA is a mathematical program with complementarity constraints (MPCC), a class of problems difficult to solve (see, e.g., Luo et al., 1996). The problem is non-convex and standard stationarity conditions such as the KKT conditions may not hold for it (Scheel and Scholtes, 2000). Compounding the difficulty is that PCSA also contains integer decision variables, which, however, can be replaced by another set of complementarity constraints (e.g., Zhang et al., 2009). Thus, our reformulation of PCSA is a regular MPCC with no integer variables.

More specifically, let W denote the smallest integer number such that $I \leq 2^W - 1$, and thus the number of charging stations allocated to node s can be represented as $y^s = \sum_{w=1}^W y_w^s 2^{w-1}$ where y_w^s is a binary variable for $w = 1, \dots, W$. However, our reformulation of PCSA treats y_w^s as a continuous decision variable and introduces instead another complementarity constraint of the form: $y_w^s(1 - y_w^s) = 0$. When combined with $0 \leq y_w^s \leq 1$, the previous equation forces y_w^s to be binary. Therefore, our reformulation of PCSA is a regular MPCC, which can be solved by many existing algorithms (see, e.g., Luo et al., 1996, and references cited therein). However, some of these algorithms only work well for small and medium problems while others, especially those based on solving equivalent non-linear programs (e.g., Fletcher and Leyffer, 2004 and Lawphongpanich and Yin, 2010), can handle larger problems.

If the number of potential allocation plans is limited, PCSA can be solved by simply solving NEP associated with each plan and then comparing their resulting social welfare. However, if the number of plans is prohibitively large, an effective solution algorithm is needed. Note that PCSA has a similar mathematical structure as a discrete equilibrium network design problem, which can be solved using an active-set algorithm (Zhang et al., 2009; Lou et al., 2009). When applied to the allocation model, the algorithm will iteratively solve NEP associated with a given allocation plan, and then construct a binary knapsack problem to update the plan. To tailor the active-set algorithm to PCSA, we define three new sets, Ω , Ω_0 and Ω_1 with $\Omega = (s, w)$, $s \in S_p$, $w = 1, \dots, W$; $\Omega_0 \cup \Omega_1 = \Omega$; $\Omega_0 \cap \Omega_1 = \emptyset$. Based on the sets, a restricted version of PCSA, i.e., RPCSA, can be formulated as follows:

$$\begin{aligned} \max_{(y, x, v, q, g, f, \delta, \rho, \tau, \kappa, p, \varpi, \theta, \zeta)} \quad & \frac{1}{\gamma} \sum_{r \in R} \ln \left(\sum_{s \in S} \exp \left[-\alpha(\rho_r^{rs} - \rho_s^{rs}) + \beta^s \left(\sum_{w=1}^W y_w^s 2^{w-1} + y_c^s \right) - \gamma p^s e^{rs} + \theta^s \right] \right) \cdot d^r \\ & + \sum_{r \in R} \sum_{s \in S} q^{rs} p^s e^{rs} - \sum_k c_k(g_k) - \sum_{s \in S} M^s \sum_{w=1}^W y_w^s 2^{w-1} \\ \text{s.t.} \quad & (1)–(14), (16)–(25) \\ & \frac{1}{\alpha} \left(\ln q^{rs} + \gamma p^s e^{rs} - \beta^s \left(\sum_{w=1}^W y_w^s 2^{w-1} + y_c^s \right) - \theta^s \right) + \rho_r^{rs} - \rho_s^{rs} - \tau^r = 0 \\ & \forall r \in R, s \in S \end{aligned} \quad (33)$$

$$\sum_{s \in S_p} \sum_{w=1}^W y_w^s 2^{w-1} \leq I \quad (34)$$

$$\sum_{s \notin S_p} \sum_{w=1}^W y_w^s 2^{w-1} = 0 \quad (35)$$

$$y_w^s = 0 \quad \forall (s, w) \in \Omega_0 \quad (36)$$

$$y_w^s = 1 \quad \forall (s, w) \in \Omega_1 \quad (37)$$

Note that RPCSA is another mathematical program with complementarity constraints, but its optimal solution can be easily obtained by solving NEP with an allocation plan compatible with (Ω_0^1, Ω_1^1) . The procedure of the active-set algorithm is described below:

- Step 0: Set $n = 1$, $\Omega_0^1 = \Omega$, and $\Omega_1^1 = \phi$. Solve NEP with a plan vector y compatible with the pair (Ω_0^1, Ω_1^1) .
- Step 1: Using the results from NEP, construct a solution $(x, y, v, q, g, f, \delta, \rho, \tau, \kappa, p, \varpi, \theta, \zeta)^T$ to RPCSA with (Ω_0^n, Ω_1^n) . Then, determine $\lambda_{s,w}^n$ and $\mu_{s,w}^n$, the smallest and largest values of Lagrangian multipliers associated with constraints (36) and (37). Set B^n as the social welfare associated with the current plan, and go to Step 2.
- Step 2: Set $Q = +\infty$ and adjust the active sets by performing the following steps:

(a) Let $(z^*, h^*)^T$ solve the following knapsack problem for plan adjustment:

$$\begin{aligned} \max \quad & \sum_{(s,w) \in \Omega_0^n} \lambda_{s,w}^n z_{s,w} - \sum_{(s,w) \in \Omega_1^n} \mu_{s,w}^n h_{s,w} \\ \text{s.t.} \quad & \sum_{(s,w) \in \Omega_1^n} y_w^s 2^{w-1} + \sum_{(s,w) \in \Omega_0^n} z_{s,w} 2^{w-1} - \sum_{(s,w) \in \Omega_1^n} h_{s,w} 2^{w-1} \leq I \\ & \sum_{(s,w) \in \Omega_0^n} \lambda_{s,w}^n z_{s,w} - \sum_{(s,w) \in \Omega_1^n} \mu_{s,w}^n h_{s,w} \leq Q \\ & z_{s,w}, h_{s,w} \in \{0, 1\} \end{aligned}$$

If the optimal objective value of the knapsack problem is zero, stop and the current solution is optimal. Otherwise, go to Step 2b.

(b) Set

$$\text{i. } P = \sum_{(s,w) \in \Omega_0^n} \lambda_{s,w}^n z_{s,w}^* - \sum_{(s,w) \in \Omega_1^n} \mu_{s,w}^n h_{s,w}^*$$

$$\text{ii. } \Omega'_0 = \left(\Omega_0^n - \left\{ (s, w) \in \Omega_0^n : z_{s,w}^* = 1 \right\} \right) \cup \left\{ (s, w) \in \Omega_1^n : h_{s,w}^* = 1 \right\}$$

$$\text{iii. } \Omega'_1 = \left(\Omega_1^n - \left\{ (s, w) \in \Omega_1^n : h_{s,w}^* = 1 \right\} \right) \cup \left\{ (s, w) \in \Omega_0^n : z_{s,w}^* = 1 \right\}$$

(c) Solve NEP with a plan vector y' compatible with (Ω'_0, Ω'_1) and calculate its social welfare denoted as B' . If $B^n < B'$, go to Step 2d because the pair (Ω'_0, Ω'_1) leads to an increase in social welfare. Otherwise, set $Q = P - \varepsilon$, where $\varepsilon > 0$ is sufficiently small, and return to Step 2a.

(d) Set $\Omega_0^{n+1} = \Omega'_0$, $\Omega_1^{n+1} = \Omega'_1$, and $n = n + 1$. Go to Step 1.

For simplicity, the initial active pair (Ω_0^1, Ω_1^1) in Step 0 corresponds to allocating no charging station. The pair corresponding to another feasible plan would certainly work. In Step 1, finding the largest and smallest Lagrangian multipliers is time consuming. In our numerical example reported in the next section, we used commercial non-linear solver such as CONOPT (Drud, 1994) to directly solve RPCSA with the solution constructed from solving NEP being the initial solution. The multipliers generated by CONOPT worked very well.

The objective of the plan adjustment problem at Step 2a is to maximize the total estimated increase to social welfare by adjusting the current allocation plan, where $z_{s,w} = 1$ means shifting (s, w) from Ω_0^n to Ω_1^n and analogously, $h_{s,w} = 1$ means the opposite. If the optimal objective value is zero, then no adjustment leads to a higher social welfare, a criterion used to terminate the algorithm above. Otherwise, an updated plan y' compatible with (Ω'_0, Ω'_1) is obtained in Step 2b. Because the Lagrangian multipliers are only estimates of the changes, y' may not lead to an actual increase in social welfare. Step 2c is to verify it by solving NEP with y' . If y' does not lead to an actual increase, the next “best” adjustment plan can be obtained by solving the plan adjustment problem in Step 2a with $Q = \sum_{(s,w) \in \Omega_0^n} \lambda_{s,w}^n z_{s,w}^* - \sum_{(s,w) \in \Omega_1^n} \mu_{s,w}^n h_{s,w}^* - \varepsilon$. Zhang et al. (2009) proved that the above active-set algorithm terminates after a finite number of iterations. The solution is strongly stationary solution if some assumptions are satisfied.

4. Numerical example

The allocation problem is solved for a coupled network that we created based on the topology of the Sioux Falls road network and a subset of the IEEE 118-bus system (<http://motor.ece.iit.edu/Data>), as shown in Fig. 2. The transportation network consists of 76 directed links and 24 nodes, 12 of which are origins and destinations. Note that although the network has the same topology as the Sioux Falls network, it has been scaled up to represent a regional network whose free-flow travel time and capacity of each link are reported in Table 1. Table 2 presents the trip production at each origin. The power network is composed of 16 transmission lines (undirected links) and 12 buses (nodes), each of which is connected to a destination node. For the DC power flow model, the base apparent power is 100 MVA. Table 3 lists the upper limit on magnitude of real power flow in each branch and its B value, i.e., the inverse of the pu reactance. The total generation cost function at each bus is assumed as follows:

$$c_k(g_k) = a_{k,2} \cdot g_k^2 + a_{k,1} \cdot g_k + a_{k,0}$$

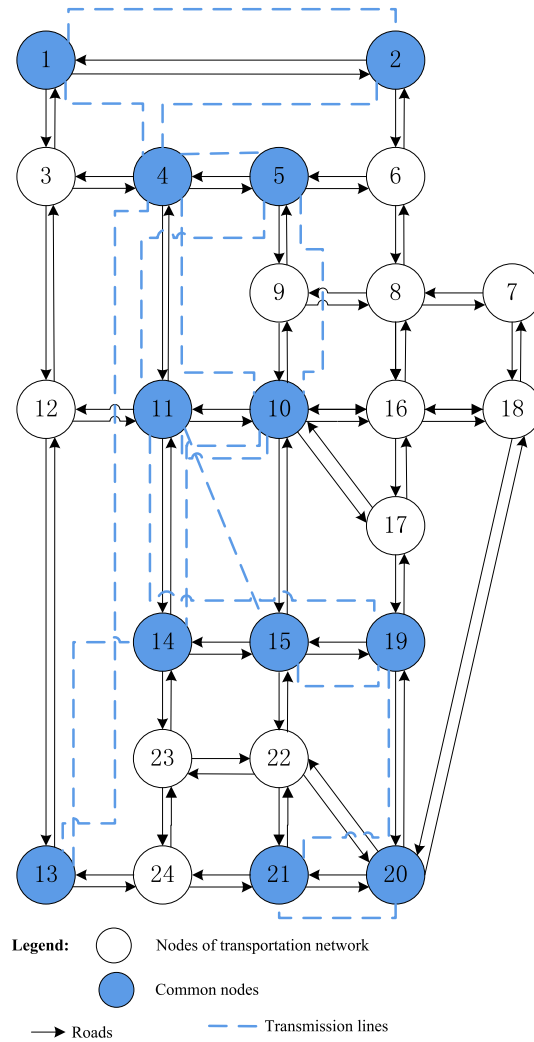


Fig. 2. The coupled transportation and power networks.

where $a_{k,2}$ (\$/MW²h), $a_{k,1}$ (\$/MWh), and $a_{k,0}$ (\$/h) are coefficients, which are given in Table 4 as well as the lower and upper limits on real power production of each generator. Other parameters include $\alpha = 1$, $\beta^s = 0.4$, $\gamma = 0.1$, $y_c^s = 3$ and $\theta^s = 0$ in the logit-based destination choice model and e^{rs} , the average hourly energy requirement for charging a PHEV, equals 8.25 kW h. Moreover, in allocating the charging stations, we did not consider their construction costs.

In this numerical example, we assumed that there are three existing charging stations at each city, and then allocated additional 20 charging stations to five potential nodes in the coupled network, i.e., nodes 1, 2, 4, 5 and 10. We assumed that at most seven charging stations can be allocated to each node, and applied the active-set algorithm to solve the allocation model. With allocating no charging stations being the initial solution, we obtained a solution of allocating seven stations at node 4, six at node 5 and seven at node 10, which yields a social welfare of 317,650. The corresponding traffic and power link flows are reported in Tables 5 and 6 respectively. Table 7 lists the LMP at each bus together with its real power injection and the power load generated by PHEVs. It can be observed from the table that the power load created by PHEV is 16% of the total power injection in the power network.

In order to verify the effectiveness of the active-set algorithm, we enumerated all possible allocation plans, i.e., 2226, and then solved the corresponding NEP for each of them and found the optimal allocation plan with the largest social welfare. Indeed, the best solution we obtained from using the active-set algorithm is the global optimal allocation plan. In addition, we observed in our numerical experiments that the active-set algorithm was very efficient and consistently produced good results with different initial solutions. The observation is consistent with Zhang et al. (2009), demonstrating the potential of applying the active-set algorithm to large-scale networks where the number of allocation plans is prohibitively large and the enumeration method fails. However, we did not prepare such a large-scale example in this paper because the focus here is not on the computational aspect.

Table 1Link capacity (10^2 veh/h) and free-flow travel time (h).

| Link | Free-flow travel time | Capacity | Link | Free-flow travel time | Capacity | Link | Free-flow travel time | Capacity |
|------|-----------------------|----------|-------|-----------------------|----------|-------|-----------------------|----------|
| 1–2 | 1.8 | 6.02 | 10–11 | 1.5 | 20 | 17–16 | 0.6 | 10.46 |
| 1–3 | 1.2 | 9.01 | 10–15 | 1.8 | 27.02 | 17–19 | 0.6 | 9.65 |
| 2–1 | 1.8 | 12.02 | 10–16 | 1.5 | 10.27 | 18–7 | 0.6 | 46.81 |
| 2–6 | 1.5 | 15.92 | 10–17 | 2.1 | 9.99 | 18–16 | 0.9 | 39.36 |
| 3–1 | 1.2 | 46.81 | 11–4 | 1.8 | 9.82 | 18–20 | 1.2 | 8.11 |
| 3–4 | 1.2 | 34.22 | 11–10 | 1.5 | 20 | 19–15 | 1.2 | 4.42 |
| 3–12 | 1.2 | 46.81 | 11–12 | 1.8 | 9.82 | 19–17 | 0.6 | 9.65 |
| 4–3 | 1.2 | 25.82 | 11–14 | 1.2 | 9.75 | 19–20 | 1.2 | 10.01 |
| 4–5 | 0.6 | 28.25 | 12–3 | 1.2 | 46.81 | 20–18 | 1.2 | 8.11 |
| 4–11 | 1.8 | 9.04 | 12–11 | 1.8 | 9.82 | 20–19 | 1.2 | 6.05 |
| 5–4 | 0.6 | 46.85 | 12–13 | 0.9 | 51.80 | 20–21 | 1.8 | 10.12 |
| 5–6 | 1.2 | 13.86 | 13–12 | 0.9 | 51.80 | 20–22 | 1.5 | 10.15 |
| 5–9 | 1.5 | 10.52 | 13–24 | 1.2 | 10.18 | 21–20 | 1.8 | 10.12 |
| 6–2 | 1.5 | 9.92 | 14–11 | 1.2 | 9.75 | 21–22 | 0.6 | 10.46 |
| 6–5 | 1.2 | 9.90 | 14–15 | 1.5 | 10.26 | 21–24 | 0.9 | 9.77 |
| 6–8 | 0.6 | 21.62 | 14–23 | 1.2 | 9.85 | 22–15 | 1.2 | 20.63 |
| 7–8 | 0.9 | 15.68 | 15–10 | 1.8 | 27.02 | 22–20 | 1.5 | 10.15 |
| 7–18 | 0.6 | 46.81 | 15–14 | 1.5 | 10.26 | 22–21 | 0.6 | 10.46 |
| 8–6 | 0.6 | 9.80 | 15–19 | 1.2 | 9.64 | 22–23 | 1.2 | 10 |
| 8–7 | 0.9 | 15.68 | 15–22 | 1.2 | 20.63 | 23–14 | 1.2 | 9.85 |
| 8–9 | 1 | 10.10 | 16–8 | 1.5 | 10.09 | 23–22 | 1.2 | 10 |
| 8–16 | 1.5 | 10.09 | 16–10 | 1.5 | 10.27 | 23–24 | 0.6 | 10.16 |
| 9–5 | 1.5 | 20 | 16–17 | 0.6 | 10.46 | 24–13 | 1.2 | 11.38 |
| 9–8 | 1 | 10.10 | 16–18 | 0.9 | 39.36 | 24–21 | 0.9 | 9.77 |
| 9–10 | 0.9 | 27.83 | 17–10 | 2.1 | 9.99 | 24–23 | 0.6 | 10.16 |
| 10–9 | 0.9 | 27.83 | | | | | | |

Table 2Trip production at each origin (10^2 veh/h).

| Origin | 1 | 2 | 4 | 5 | 10 | 11 | 13 |
|------------|-------|-------|-------|-------|-------|-------|-------|
| Production | 12.92 | 12.71 | 12.18 | 12.51 | 13.51 | 13.41 | 11.46 |
| Origin | 14 | 15 | 19 | 20 | 21 | | |
| Production | 13.20 | 14.11 | 13.31 | 11.70 | 11.93 | | |

Table 3

Input data for transmission lines.

| Line | Capacity (MW) | B | Line | Capacity (MW) | B |
|-------|---------------|-------|-------|---------------|-------|
| 1–2 | 175 | 66.23 | 4–13 | 500 | 25.91 |
| 2–4 | 175 | 3.98 | 13–14 | 500 | 50 |
| 1–4 | 175 | 4.63 | 10–14 | 500 | 37.31 |
| 4–5 | 175 | 6.90 | 11–15 | 175 | 4.59 |
| 4–10 | 175 | 6.67 | 11–19 | 175 | 8.55 |
| 5–10 | 500 | 74.07 | 15–19 | 175 | 9.85 |
| 5–11 | 175 | 17.83 | 19–21 | 175 | 3.60 |
| 10–11 | 175 | 26.60 | 20–21 | 500 | 27.03 |

Table 4

Input data for generators.

| At node | Load (MW) | Lower limit (MW) | Upper limit (MW) | a_2 (10^{-2}) | a_1 | a_0 |
|---------|-----------|------------------|------------------|---------------------|-------|-------|
| 1 | 63 | 25 | 100 | 1.28 | 17.82 | 10.15 |
| 2 | 84 | 25 | 100 | 1.28 | 17.82 | 10.15 |
| 4 | 277 | 50 | 200 | 1.39 | 13.29 | 39 |
| 5 | 78 | 0 | 0 | 0 | 0 | 0 |
| 10 | 0 | 50 | 200 | 1.39 | 13.29 | 39.00 |
| 11 | 77 | 25 | 100 | 1.28 | 17.82 | 10.15 |
| 13 | 0 | 0 | 0 | 0 | 0 | 0 |
| 14 | 0 | 0 | 0 | 0 | 0 | 0 |
| 15 | 39 | 100 | 420 | 1.36 | 8.34 | 64.16 |
| 19 | 28 | 0 | 0 | 0 | 0 | 0 |
| 20 | 0 | 0 | 0 | 0 | 0 | 0 |
| 21 | 0 | 80 | 300 | 1.09 | 12.89 | 6.78 |

Table 5
Traffic link flow (veh/h).

| Link | Flow | Link | Flow | Link | Flow |
|------|---------|-------|---------|-------|--------|
| 1–2 | 180.67 | 10–11 | 178.48 | 17–16 | 292.76 |
| 1–3 | 1119.94 | 10–15 | 113.74 | 17–19 | 48.41 |
| 2–1 | 153.64 | 10–16 | 27.79 | 18–7 | 168.10 |
| 2–6 | 1158.08 | 10–17 | 25.81 | 18–16 | 421.39 |
| 3–1 | 69.69 | 11–4 | 969.50 | 18–20 | 26.94 |
| 3–4 | 1866.17 | 11–10 | 1375.07 | 19–15 | 335.17 |
| 3–12 | 46.42 | 11–12 | 26.99 | 19–17 | 830.17 |
| 4–3 | 33.11 | 11–14 | 136.92 | 19–20 | 282.69 |
| 4–5 | 1911.90 | 12–3 | 829.23 | 20–18 | 589.49 |
| 4–11 | 57.18 | 12–11 | 262.19 | 20–19 | 376.36 |
| 5–4 | 2071.02 | 12–13 | 56.98 | 20–21 | 225.37 |
| 5–6 | 20.16 | 13–12 | 1074.98 | 20–22 | 20.21 |
| 5–9 | 313.81 | 13–24 | 185.32 | 21–20 | 195.73 |
| 6–2 | 43.79 | 14–11 | 1095.64 | 21–22 | 705.63 |
| 6–5 | 1116.93 | 14–15 | 202.70 | 21–24 | 361.92 |
| 6–8 | 313.40 | 14–23 | 91.71 | 22–15 | 705.63 |
| 7–8 | 168.10 | 15–10 | 1550.92 | 22–20 | 13.97 |
| 7–18 | 11.44 | 15–14 | 156.49 | 22–21 | 85.13 |
| 8–6 | 295.88 | 15–19 | 250.04 | 22–23 | 20.21 |
| 8–7 | 11.44 | 15–22 | 85.13 | 23–14 | 149.81 |
| 8–9 | 291.66 | 16–8 | 116.36 | 23–22 | 13.97 |
| 8–16 | 10.30 | 16–10 | 597.79 | 23–24 | 77.74 |
| 9–5 | 1111.21 | 16–17 | 22.60 | 24–13 | 305.16 |
| 9–8 | 11.42 | 16–18 | 15.49 | 24–21 | 190.21 |
| 9–10 | 605.47 | 17–10 | 537.41 | 24–23 | 129.60 |
| 10–9 | 1122.63 | | | | |

Table 6
Power line flow (MW).

| Line | Flow | Line | Flow |
|-------|---------|-------|---------|
| 1–2 | 13.44 | 4–13 | –123.12 |
| 2–4 | –47.08 | 13–14 | –125.17 |
| 1–4 | –53.21 | 10–14 | 128.25 |
| 4–5 | –68.37 | 11–15 | –140.81 |
| 4–10 | –71.66 | 11–19 | –175 |
| 5–10 | –58.27 | 15–19 | 98.23 |
| 5–11 | –112.74 | 19–21 | –109.31 |
| 10–11 | –147.56 | 20–21 | –3.94 |

Table 7
PHEV load, power injection and LMP at each bus.

| At node | PHEVs' load (MW) | Power injection (MW) | LMP (\$/MWh) |
|---------|------------------|----------------------|--------------|
| 1 | 1.77 | 25 | 17.4 |
| 2 | 1.52 | 25 | 17.4 |
| 4 | 34.01 | 148.14 | 17.4 |
| 5 | 24.63 | 0 | 17.4 |
| 10 | 37.53 | 148.14 | 17.4 |
| 11 | 3.51 | 25 | 17.4 |
| 13 | 2.04 | 0 | 17.4 |
| 14 | 3.08 | 0 | 17.4 |
| 15 | 5.99 | 284.03 | 16.06 |
| 19 | 4.60 | 0 | 15.43 |
| 20 | 3.94 | 0 | 15.43 |
| 21 | 3.55 | 116.87 | 15.43 |

Fig. 3 plots the cumulative distribution curve of the social welfare of those 2226 possible allocation plans. It can be observed that the social welfare varies approximately from 210,000 and 320,000, and many plans fall into the range between 230,000 and 290,000. Such a dispersed distribution highlights the importance of making a wise allocation decision and the need for an optimal allocation model. In Table 8, we further compare the LMPs corresponding to the best allocation plan obtained from using the active-set algorithm with those corresponding to two randomly selected plans, and the situation

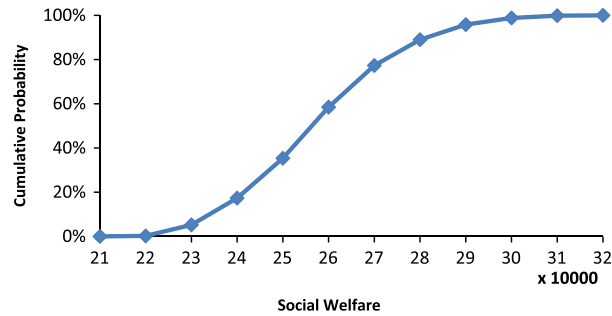


Fig. 3. Cumulative distribution curve of social welfare.

Table 8

LMPs associated with different allocation plans (\$/MWh).

| At node | Without PHEVs | Best plan obtained | Randomly selected plan 1 | Randomly selected plan 2 |
|----------------|---------------|--------------------|--------------------------|--------------------------|
| 1 | 15.96 | 17.40 | 17.20 | 17.30 |
| 2 | 15.96 | 17.40 | 17.20 | 17.30 |
| 4 | 15.96 | 17.40 | 17.20 | 17.30 |
| 5 | 15.96 | 17.40 | 17.20 | 17.30 |
| 10 | 15.96 | 17.40 | 17.20 | 17.30 |
| 11 | 15.96 | 17.40 | 17.20 | 17.30 |
| 13 | 15.96 | 17.40 | 17.20 | 17.30 |
| 14 | 15.96 | 17.40 | 17.20 | 17.30 |
| 15 | 15.55 | 16.06 | 16.15 | 16.11 |
| 19 | 15.36 | 15.43 | 15.66 | 15.55 |
| 20 | 15.36 | 15.43 | 15.66 | 15.55 |
| 21 | 15.36 | 15.43 | 15.66 | 15.55 |
| Social welfare | – | 317,650 | 232,436 | 253,317 |

without newly allocated charging stations. The first randomly selected plan allocates four charging stations at node 1, seven at node 2, four at node 4 and five at node 5, and the other allocates one at node 1, five at node 2, four at node 4, five at node 5 and five at node 10. It can be observed that the PHEV loads have substantial impacts on the prices of electricity and the impacts are very sensitive to the allocation decisions. Finally, it is easy to observe that the best obtained plan allocates public charging stations in three cities whereas two randomly selected plans allocate stations in four or five cities. One may favor the latter because they serve more cities. If it is the intent to find a plan to ensure certain coverage for equity or social justice, additional constraints can be introduced to the formulation to guarantee that, e.g., the number of charging stations at each city should be more than a certain threshold or the number of cities served should be larger than a threshold.

5. Conclusions

We have adopted a game theoretical approach to investigate the interactions among availability of public charging opportunities, destination and route choices of PHEVs and price of electricity in coupled transportation and power networks. The interactions lead to an equilibrium where equilibrium prices of electricity, and traffic and power flow distributions can be determined. A convex mathematical program is formulated to describe the equilibrium state. Built upon the proposed equilibrium analysis framework, the problem of optimally allocating public charging stations is formulated as a mathematical program with complementarity constraints, and is solved by an active-set algorithm. It is observed from the numerical example that the charging load from PHEVs has substantial impact on the operations of the power network and the price of electricity. Consequently, it is important to consider this impact when allocating public charging stations. The proposed location model will be of help to government agencies for deployment planning of public charging infrastructure. The active-set algorithm has been demonstrated to be effective and efficient.

The proposed model in this paper is based on a critical assumption that availability of public charging stations and prices of electricity will affect destination choices of PHEVs. This assumption needs to be verified by future empirical studies. As one of the first attempts to analyze the coupled power and transportation networks, this paper has adopted a static modeling framework. It is certainly necessary and useful to extend this static framework to be time dependent, considering time-varying demands of travel and electricity, and capturing the temporal difference of LMPs of electricity. Although the extension work appears to be a major undertaking since it integrates a dynamic traffic assignment model (e.g., Peeta and Ziliaskopoulos, 2001) with a time-dependent power flow model (e.g., Wang et al., 2010), the principles of equilibrium analysis

proposed in this paper still apply. Moreover, the extended allocation model would possess a similar mathematical structure as its static counterpart in this paper.

Acknowledgements

The authors thank three anonymous reviewers for their helpful comments. This research was partly funded by National Science Foundation (CNS-1239364) and National Natural Science Foundation of China (71228101). The authors also wish to thank Dr. Jianhui Wang at Argonne National Laboratory for his insights on the power network operations.

References

- Bertsekas, D.P., 2003. Nonlinear Programming. Athena Scientific, Belmont, MA.
- Bradley, T.H., Frank, A.A., 2009. Design, demonstration and sustainability impact assessments for plug-in hybrid electric vehicles. *Renewable and Sustainable Energy Reviews* 13 (1), 115–128.
- Davies, J., Kurani, K.S., 2010. Estimating marginal impact of workplace charging on electricity demand and charging depleting driving. Scenarios based on plausible early market commuters' use of a 5 kW h conversion PHEV. Compendium of Papers DVD of TRB 90th Annual Meeting, Transportation Research Board.
- Drud, A., 1994. CONOPT – a large scale GRG code. *ORSA Journal on Computing* 6 (2), 207–216.
- Feldman, P., 2012. A day in the life of the grid: July 21, 2011. Presentation at the Winter Committee Meeting of National Association of Regulatory Utility Commissioners, Washington DC. <<http://www.narucmeetings.org/Presentations/PaulFeldmanMISOPPT.pdf>>.
- FERC, 2003. Notice of White Paper, US Federal Energy Regulatory Commission, Issued April 28.
- Fox News, 2012. <<http://www.foxnews.com/travel/2012/01/31/are-electric-car-charging-stations-new-must-have-hotel-amenity/>> (accessed 28.06.12).
- Frade, I., Ribeiro, A., Goncalves, G., Antunes, A.P., 2010. An optimization model for locating electric vehicle charging stations in central urban areas. Compendium of Papers DVD of TRB 90th Annual Meeting, Transportation Research Board.
- Fletcher, R., Leyffer, S., 2004. Solving mathematical program with complementarity constraints for nonlinear programs. *Optimization Methods and Software* 19 (1), 15–40.
- Galus, M.D. and Andersson, G., 2008. Demand management of grid connected plug-in hybrid electric vehicles. IEEE Energy 2030 Conference, <http://dx.doi.org/10.1109/ENERGY.2008.4781014>.
- GLOBE-Net, 2012. <<http://www.globe-net.com/articles/2012/april/9/bc-plan-for-electric-car-charging-stations-may-unleash-vehicles-around-province/>> (accessed 28.06.12).
- IEEE, 2007. Plug-in Electric Hybrid Vehicles. Position Statement of IEEE-USA Board of Directors.
- Ip, A., Fong, S., Liu, E., 2010. Optimization for allocating BEV recharging stations in urban areas by using hierarchical clustering. In: Proceedings of 6th International Conference on Advanced Information Management and Service, pp. 460–465.
- Lewis, G.McD., 2010. Estimating the value of wind energy using electricity locational marginal price. *Energy Policy* 38 (7), 3221–3231.
- Kalhammer, F.R., Kamath, H., Duvall, M., Alexander, M., Jungers, B., 2009. Plug-in hybrid electric vehicles: promise, issues and prospects. EVS24 International Battery, Hybrid and Fuel Cell Electric Vehicle Symposium, Stavanger, Norway, May 13–16.
- Kemperman, A., Borgers, A., Timmermans, H., 2002. Incorporating variety-seeking and seasonality in stated preference modeling of leisure trip destination choice: a test of external validity. *Transportation Research Record* 1807, 67–76.
- Kezunovic, M., Waler, S.T., Damjanovic, I., 2010. Framework for studying emerging policy issues associated with PHEVs in managing coupled power and transportation systems. In: 2010 IEEE Green Technologies Conference, <http://dx.doi.org/10.1109/GREEN.2010.5453787>.
- Kitamura, R., Sperling, D., 1987. Refueling behavior of automobile drivers. *Transportation Research Part A* 21 (3), 235–245.
- Lawphongpanich, S., Yin, Y., 2010. Solving Pareto-improving congestion pricing for general road networks. *Transportation Research Part C* 18 (2), 234–246.
- Lin, Z., Greene, D.L., 2011. Promoting the market for plug-in hybrid and battery electric vehicles: the role of recharge availability. *Transportation Research Record* 2252, 49–56.
- Litvinov, E., Zheng, T., Rosenwald, G., Shamsollahi, P., 2004. Marginal loss modeling in LMP calculation. *IEEE Transactions on Power Systems* 19 (2), 880–888.
- Lou, Y., Yin, Y., Lawphongpanich, S., 2009. Robust approach to discrete network designs with demand uncertainty. *Transportation Research Record* 2090, 86–94.
- Luo, Z.-Q., Pang, J.-S., Ralph, D., 1996. Mathematical Programs with Equilibrium Constraints. Cambridge University Press, New York, New York.
- Markel, T., 2010. Plug-in electric vehicle infrastructure: a foundation for electrified transportation. Paper Presented at the MIT Energy Initiative Transportation Electrification Symposium, Cambridge, Massachusetts. NREL/CP-540-47951.
- Morrow, K., Karner, D., Francfort, J., 2008. Plug-in Hybrid Electric Vehicle Charging Infrastructure Review. Final Report to US Department of Energy Vehicle Technologies Program – Advanced Vehicle Testing Activity.
- Obama, B., 2008. Energy Speech Fact Sheet. <http://www.barackobama.com/pdf/factsheet_energy_speech_080308.pdf>.
- Overbye, T., Cheng, X., Sun, Y., 2004. A comparison of the AC and DC power flow models for LMP calculation. In: Proceedings of the 37th Hawaii International Conference on System Sciences.
- Pan, F., Bent, R., Berscheid, A., Izraelevitz, D., 2010. Locating PHEV exchange stations in V2G. In: Proceedings of 1st IEEE International Conference on Smart Grid Communications (SmartGridComm), pp. 173–178.
- Peeta, S., Ziliaskopoulos, A., 2001. Foundations of dynamic traffic assignment: the past, the present, and the future. *Networks and Spatial Economics* 1 (3–4), 233–265.
- Rotering, N., Ilic, M., 2011. Optimal charge control of plug-in hybrid electric vehicles in deregulated electricity markets. *IEEE Transactions on Power Systems* 26 (3), 1021–1029.
- Scheel, H., Scholtes, S., 2000. Mathematical programs with complementarity constraints: stationarity, optimality, and sensitivity. *Mathematics of Operations Research* 25 (1), 1–22.
- Sheffi, Y., 1984. Urban Transportation Networks: Equilibrium Analysis with Mathematical Programming Methods. Prentice-Hall, Inc., Englewood Cliffs, NJ.
- Sioshansi, R., 2012. Modeling the impacts of electricity tariffs on plug-in hybrid electric vehicle charging, costs, and emissions. *Operations Research*, doi:<http://dx.doi.org/10.1287/opre.1120.1038>.
- Southworth, F., 1981. Calibration of multinomial logit models of mode and destination choice. *Transportation Research Part A* 15 (4), 315–325.
- Sun, J., Tesfatsion L., 2010. DC optimal power flow formulation and solution using QuadProgJ. Working Paper No. 06014, Iowa State University.
- Sweda, T., Klabjan, D., 2011. An agent-based decision support system for electric vehicle charging infrastructure deployment. In: 7th IEEE Vehicle Power and Propulsion Conference, Chicago, Illinois.
- Tuttle, D.P., Kockelman, K.M., 2012. Electrified vehicle technologies: trends, infrastructure implications and cost comparisons. *Journal of the Transportation Research Forum* 51 (1), 35–51.
- Walsh, K., Enz, C., Canina, L., 2004. The impact of gasoline price fluctuations on loading demand for US brand hotels. *International Journal of Hospitality* 23 (5), 505–521.
- Wang, J., Liu, C., Ton, D., Zhou, Y., Kim, J., Vyas, A., 2011. Impact of plug-in hybrid electric vehicles on power systems with demand response and wind power. *Energy Policy* 39 (7), 4016–4021.

- Wang, L., Lin, A., Chen, Y., 2010. Potential impact of recharging plug-in hybrid electric vehicles on locational marginal prices. *Naval Research Logistics* 57 (8), 686–700.
- Wehinger, L.A., Galus, M.D., Andersson, G., 2010. Agent-based simulator for the German electricity wholesale market including wind power generation and widescale PHEV adoption. In: 7th International Conference on the European Energy Market, <http://dx.doi.org/10.1109/EEM.2010.5558718>.
- Weis, C., Axhausen, K.W., Schlich, R., Zbinden, R., 2010. Models of mode choice and mobility tool ownership beyond 2008 fuel prices. *Transportation Research Record* 2157, 86–94.
- Zhang, L., Lawphongpanich, S., Yin, Y., 2009. An active-set algorithm for discrete network design problems. *Transportation and Traffic Theory 2009: Golden Jubilee 2009*, 283–300.